

EXHIBIT 3

Very high growth rate chemical vapor deposition of single-crystal diamond

Chih-shiue Yan*, Yogesh K. Vohra†, Ho-kwang Mao*, and Russell J. Hemley**

*Geophysical Laboratory, Carnegie Institution of Washington, 5251 Broad Branch Road NW, Washington, DC 20015; and †Department of Physics, University of Alabama, Birmingham, AL 35294

Contributed by Russell J. Hemley, August 2, 2002

Diamond possesses extraordinary material properties, a result that has given rise to a broad range of scientific and technological applications. This study reports the successful production of high-quality single-crystal diamond with microwave plasma chemical vapor deposition (MPCVD) techniques. The diamond single crystals have smooth, transparent surfaces and other characteristics identical to that of high-pressure, high-temperature synthetic diamond. In addition, the crystals can be produced at growth rates from 50 to 150 $\mu\text{m}/\text{h}$, which is up to 2 orders of magnitude higher than standard processes for making polycrystalline MPCVD diamond. This high-quality single-crystal MPCVD diamond may find numerous applications in electronic devices as high-strength windows and in a new generation of high-pressure instruments requiring large single-crystal anvils.

Diamond produced by low-pressure microwave plasma (MP) chemical vapor deposition (CVD) is the most promising technology for producing low-cost and high-quality large diamond (1, 2). Nevertheless, the widespread use of MPCVD diamond in many applications has not been successful due to the existence of grain boundaries of polycrystalline diamond that are produced and slow growth rates, typically 1 $\mu\text{m}/\text{h}$ (1–7). Diamond's strong covalent bonds and rigid structure (8) give rise to its unique properties. Diamond is the hardest and stiffest material known, has the highest room-temperature thermal conductivity and one of the lowest thermal expansion of known materials, and is radiation-hard and chemically inert to most acidic and basic reagents. Due to the high cost, limited size, and uneasily controlled impurities of natural and synthetic high-pressure, high-temperature (HPHT) diamond, the applications of diamond have in fact been limited in comparison to its great potential (8). Thus, CVD diamond is the most promising avenue available for synthetic diamond. The major CVD diamond-coating techniques are the hot-filament, radio-frequency plasma, MP, and arcjet-torch methods (8, 9). Comparing these techniques, MPCVD-reactor methods provide stable conditions, reproducible sample quality, and reasonable cost (8, 9). In fact, steady progress in MPCVD synthesis techniques has made it possible to manufacture high-quality polycrystalline CVD-diamond optical components (4, 10), but this polycrystalline material consists of a patchwork of tiny crystals welded to one another along misaligned grain boundaries, which block the flow of current (10–12). The major disadvantage of MPCVD using 12.2 cm/2.54 GHz for plasma generation is the lower growth rate, typically 1 $\mu\text{m}/\text{h}$ (1–7) compared with arcjet torches; moreover at several hundred micrometers per hour (13), the plasma tends to concentrate at tips and edges (9, 13). Here we show that MPCVD diamond can be produced as high-quality and high growth rate (50–150 μm depending on stage design and methane concentration) single crystals for a variety of purposes including the enlargement of anvils (14) for compressing large samples at ultrahigh pressures.

The depositions were conducted at the University of Alabama in a 6-kW, 2.45-GHz MPCVD chamber with a volume of \approx 5,000 cm^3 (Wavemat, model MPDR313EHP, Plymouth, MI) evacuated to a base pressure of $<10^{-3}$ torr (1 torr = 133 Pa). The

cavity and substrate stage have been redesigned to sustain a stable and energetic plasma for high growth rate applications at low microwave power (1–2 kW) that also prevent plasma concentration at edges. The overall effect of the redesigned stage enhances the growth rate by a factor of 10 and reduces the microwave power by a factor of 3 compared with Wavemat's original design. The deposition temperature was measured by a two-color infrared (\approx 1.6- μm) ratio thermometer (Mikron Instruments, model M-775, Oakland, NJ); the thermal emission was focused through a quartz window at an incident angle of 65° on the target, with a 2-mm diameter minimum target size. A PC (running LABVIEW software) automatically controlled the gas mass-flow, thermometer, and microwave-power levels. The substrates were commercial 3.5 \times 3.5 \times 1.6-mm³ HPHT synthetic type Ib diamonds; the deposition surface was within 2° of the {100} top surface (Fig. 1). The substrates required polished, smooth surfaces that were cleaned ultrasonically with acetone and mechanically mounted on a molybdenum-substrate holder to ensure a uniform temperature. The deposited diamond was characterized by Raman and photoluminescence spectroscopies, electron paramagnetic resonance (EPR), and x-ray diffraction (XRD). Experimental variables including the reactant gas pressure and concentration, substrate temperature, and sample stage were varied to optimize diamond growth quality and increase {100} growth rate (15). Our previous study showed that when the reactor pressure is increased from 60 to 200 torr, the diamond growth rate increases \approx 5-fold, while penetration twins decreased (15). A small amount of nitrogen added (1–5% N₂/CH₄) to the reactive gas has been shown to have a beneficial effect of creating more available growth sites, enhancing the growth rate to three times and promoting {100} face growth (4–7). Using the published information on the optimal chemical conditions together with the redesigned stage, we thus were able to achieve growth-rate enhancements by up to 2 orders of magnitude. The experiments were performed at a pressure of 160 torr, 3% N₂/CH₄, and a high percentage of methane (12% CH₄/H₂). Under these conditions a seed produced with a 1-inch-diameter plasma, the growth morphology and color strongly depend on temperature, with the smooth, dark brown at 1,000–1,100°C, brown at 1,100–1,200°C, and tinted yellow at 1,200–1,220°C. Step flow-type with pyramid-like octahedra tinted yellow formed at 1,230–1,400°C, spherical black diamond-like carbon was produced below 1,000°C, and twinned or polycrystalline diamond resulted at over 1,300°C. The temperature range for smooth, yellow-tint growth is narrow (1,200–1,220°C) and can be missed easily; it also varies with sample size due to the 2-mm-diameter minimum target size of the thermometer and broadband plasma emission.

Under these conditions, we can produce transparent MPCVD diamond that is as smooth as the HPHT diamond seed, enlarging both the thickness and area of the crystal. Fig. 1 shows a photograph of a 3.3 \times 3.5 \times 1.6-mm³ substrate seed and

APPLIED PHYSICAL SCIENCES

Abbreviations: MP, microwave plasma; CVD, chemical vapor deposition; HPHT, high-pressure, high-temperature; XRD, x-ray diffraction.

*To whom reprint requests should be addressed. E-mail: r.hemley@gl.ciw.edu.

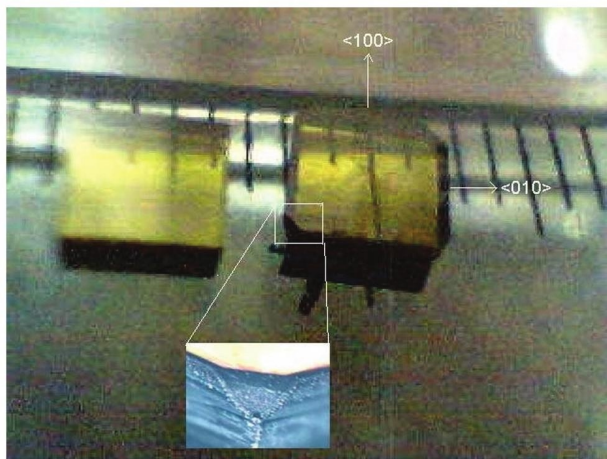


Fig. 1. Photograph of seed and as-grown unpolished CVD diamond and a magnification of CVD-diamond corner. The $\langle 100 \rangle$ direction corresponds to the four sides of the diamond cube.

as-grown CVD $4.2 \times 4.2 \times 2.3$ -mm³ unpolished diamond with a 0.7-mm deposit on the seed in a 12-h run at a growth rate of 58 $\mu\text{m}/\text{h}$ at 1,220°C and 160 torr [500 standard $\text{cm}^3\text{min}^{-1}$ (sccm) H_2 , 60 sccm CH_4 , and 1.8 sccm N_2] and microwave power of 1.6 kW. The growth morphology indicates that the $\langle 100 \rangle$ side-growth rate is faster than that of the $\langle 111 \rangle$ corner-growth rate. One can estimate the value of the growth parameter $\alpha = 3^{1/2} V_{100}/V_{111}$ (16, 17), which describes the ratio of the growth rate on $\{100\}$ and $\{111\}$ faces, at ≈ 2.5 –3.0. The optimal situation is for α to be close to 3; thus, preferential growth along the $\langle 100 \rangle$ direction can be achieved (16, 17). We have successfully produced 5-carat single crystal (dimensions, 7 \times 8 \times 5 mm) after an \approx 10-times-longer regrowth from a 0.3-mm-thick seed, but it was brown in color and had a crack on the $\{111\}$ face. This phenomenon may be due to initial atomic hydrogen etching or a hot edge that will promote a darker, discontinuous interface during regrowth, twin formation, or internal stresses (15, 18). The sharp $\{111\}$ cracking implies that our CVD diamond is a single crystal.

Fig. 2a shows the photoluminescence spectrum (laser-excitation wavelength of 514.5 nm) of seed and as-grown CVD diamond. The nitrogen-vacancy pair at 638 nm and interstitial nitrogen vacancy at 572 nm were observed in diamond with added nitrogen (19, 20) and no obvious nitrogen-related center in the seed. The intensity of nitrogen vacancy and interstitial nitrogen vacancy rises linearly with increasing added N_2 . This confirms that nitrogen is incorporated effectively into CVD diamond. The CVD and diamond type Ib seed crystals (10) exhibit comparable transmission in the visible/near-infrared range, demonstrating similar performance as optical windows (Fig. 2a Inset). Raman spectra for both the seed and the as-grown CVD diamond exhibit the strong diamond peak of 1,332.5 cm⁻¹ with the same full width at half-maximum of 3.4 cm⁻¹ (Fig. 2b). These results mean that the top surface of the CVD diamond possesses a different optical character but the same internal stress strength as the HPHT-diamond seed (21).

Our previous EPR study of CVD diamond showed that nitrogen is incorporated mainly into CVD diamond as a substitutional-nitrogen defect (P1 center), and that other various aggregate forms do not exist (15, 22). The substitution incorporation of nitrogen results in distortion of the diamond lattice and the observed transition from $\langle 111 \rangle$ -to- $\langle 100 \rangle$ growth habit in the film. This phenomenon may be related to the large unique distortion along the $\langle 111 \rangle$ direction of the C—N bond on which the unpaired electron is situated and which is 10–36% longer than the normal C—C bond (23). It can be argued qualitatively

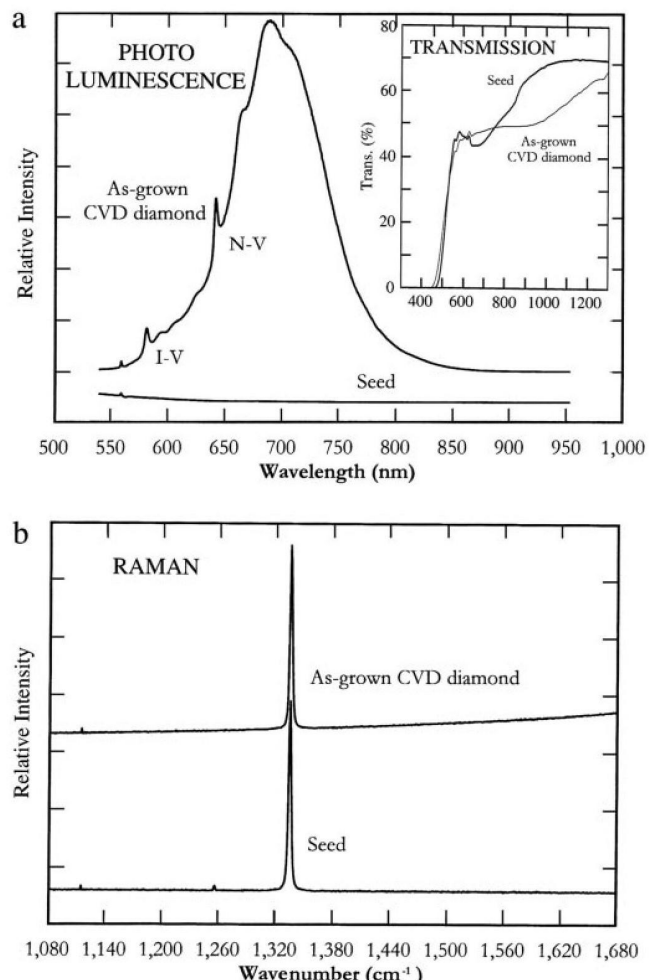


Fig. 2. (a) Photoluminescence spectra of as-grown CVD and seed diamonds. (Inset) Visible/near-infrared transmission spectra. (b) Raman spectra of the CVD and seed diamonds shown in Fig. 1.

why the $\langle 100 \rangle$ direction is favored over $\langle 111 \rangle$ (5). In our study, a concentration of P1 centers from 40 to 100 ppm was observed (15). The nitrogen (P1 center) concentration decreases with increasing temperature as a result of single-substitutional nitrogen migrating to form various types of nitrogen aggregates (24). This phenomenon is similar to that found with HPHT treatment (25).

XRD confirms that the CVD diamonds produced in this way are single crystals. XRD (400) ω scans reveal that the as-grown whole CVD diamond has a full width at half-maximum of 0.13° (Fig. 3a) as compared with a full width at half-maximum of 0.058° for the substrate (Fig. 3c). The slight broadening of grown CVD diamond indicates a small degree of polycrystallinity or twinning. We masked the top edge of the CVD diamond with a 10 \times 10 \times 0.3-mm³-thick molybdenum sheet, with only a half-center, square 3 \times 3-mm² area exposed to the x-rays. The XRD pattern (Fig. 3b) shows that the bulk of the CVD diamond has a narrow full width at half-maximum of 0.064°, which is close to that of the seed. Hence, any polycrystalline character of the CVD diamond is localized on the edge. Moreover, the corner magnification in Fig. 1 shows that considerable spherical diamond-like carbon exists on the edge and corner, but the top edge is sharp and straight. After polishing off the small amount of black diamond-like carbon, which broadens the XRD peak width, our CVD diamond is a single crystal.

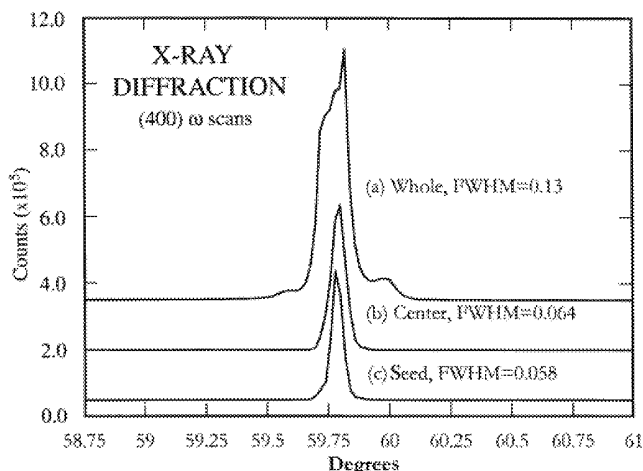


Fig. 3. XRD (400) ω scan of grown whole CVD diamond (a), center half area of CVD diamond (b), with the other part masked with a molybdenum sheet, and diamond seed (c). FWHM, full width at half-maximum.

We have also produced with the same design of the stage a high-quality 0.6-mm-thick pure-CVD single crystal by adding a small amount of oxygen and lowering the growth temperature to 800–1,000°C at 0.2–2% O₂/CH₄, 1–7% CH₄/H₂, and 160 torr. The added oxygen allows a lower growth temperature, which removes the nitrogen-related impurities and reduces the silicon

and hydrogen impurity levels (26, 27). Although this gives a lower growth rate of \approx 10 $\mu\text{m}/\text{h}$, the rate is still over 1 order of magnitude higher than that of standard processes, typically 0.3 $\mu\text{m}/\text{h}$ (26, 27). This high-quality diamond may be very useful in high-power laser window applications. We also found that yellow or brown HPHT diamond can be annealed during MPCVD growth at temperatures of 1,500°C for several hours by using a special stage design to form green diamond; this annealing results from single-substitutional nitrogen atoms migrating to form various types of nitrogen aggregates (24). This phenomenon of color enhancement (as shown in Fig. 2) is similar to HPHT treatment (25); further identification can be carried out by using infrared-absorption techniques (24, 25). For electronic applications, carrier mobility, thermal conductivity, and surface acoustic-wave velocity should be measured. One promising technique is to use HPHT treatment to fix and enhance cracked, brownish MPCVD diamond to produce colorless material.

We believe that our high growth rate technique will allow the production of large, high-quality CVD diamond. There are important implications for high-pressure research. Large, perfect single-crystal diamond anvils are required for enhancing the volume of samples that can be compressed at ultrahigh pressure. As such, the development of this synthesis technique should open up new classes of measurements such as neutron scattering and NMR in the megabar pressure range.

We are grateful to D. D. Klug and V. V. Struzhkin for comments on the manuscript. The work was supported by the National Science Foundation and the W. M. Keck Foundation.

1. Spitsyn, B. V., Bouilov, L. L. & Deryaguin, B. V. (1981) *J. Cryst. Growth* **52**, 219–226.
2. Kamo, M., Sato, Y., Matsumoto, S. & Setaka, N. (1983) *J. Cryst. Growth* **62**, 642–644.
3. Vitton, J. P., Garenne, J. J. & Truchet, S. (1993) *Diamond Relat. Mater.* **2**, 713–717.
4. Cao, G. Z., Schemer, J. J., van Enckevort, W. J. P., Elst, W. A. L. M. & Giling, L. J. (1996) *J. Appl. Phys.* **79**, 1357–1364.
5. Jin, S. & Moustakas, T. D. (1994) *Appl. Phys. Lett.* **65**, 403–405.
6. Müller-Sebert, W., Wörner, E., Fuchs, F., Wild, C. & Koidl, P. (1996) *Appl. Phys. Lett.* **68**, 759–760.
7. Afzal, A., Rego, C. A., Ahmed, W. & Cherry, R. I. (1998) *Diamond Relat. Mater.* **7**, 1033–1038.
8. Field, J. E. (1992) *The Properties of Natural and Synthetic Diamond* (Academic, London).
9. Bachmann, P. K. & Lydtn, H. (1990) in *Characterization of Plasma Process*, eds. Lukovsky, G., Ibbotson, D. E. & Hess, D. W., Materials Research Society Symposium Proceedings (Mater. Res. Soc., Warrendale, PA), Vol. 165, p. 181.
10. Sussmann, R. S. (1993) *Ind. Diamond Rev.* **53**, 63–71.
11. Jiang, X. & Jia, C. L. (1996) *Appl. Phys. Lett.* **69**, 3902–3904.
12. Schreck, M., Hörmann, H. R., Lindner, J. K. N. & Stritzker, B. (2001) *Appl. Phys. Lett.* **78**, 192–194.
13. Prelas, M. A., Popovici, G. & Bigelow, L. K. (1998) *Handbook of Industrial Diamonds and Diamond Films* (Dekker, New York) pp. 821–847.
14. Xu, J. A. & Mao, H. K. (2000) *Science* **290**, 783–785.
15. Yan, C. S. & Vohra, Y. K. (1999) *Diamond Relat. Mater.* **8**, 2022–2031.
16. Wild, C., Kohl, R., Herres, N., Müller-Sebert, W. & Koidl, P. (1994) *Diamond Relat. Mater.* **3**, 373–381.
17. Tamor, M. A. & Everson, M. P. (1994) *J. Mater. Res.* **9**, 1839–1847.
18. Stallcup, R. E. & Perez, J. M. (2001) *Phys. Rev. Lett.* **86**, 3368–3371.
19. Vohra, Y. K., Israel, A. & Catledge, S. A. (1997) *Appl. Phys. Lett.* **71**, 321–323.
20. Nijenhuis, J. T., Olsthoorn, S. M., Van Enckevort, W. J. P. & Giling, L. J. (1997) *J. Appl. Phys.* **82**, 419–422.
21. Nishitani, G. M., Sakaguchi, I., Loh, K. P., Kanda, H. & Ando, T. (1998) *Appl. Phys. Lett.* **73**, 765–767.
22. Graeff, C. F. O., Rohrer, E., Nebel, C. E. & Stutzmann, M. (1996) *Appl. Phys. Lett.* **69**, 3215–3217.
23. Loubser, J. H. N. & Wyk, J. A. (1978) *Rep. Prog. Phys.* **41**, 1201–1248.
24. Collins, A. T. (1980) *J. Phys. C Solid State Phys.* **13**, 2641–2650.
25. Collins, A. T., Kanda, H. & Kitawaki, H. (2000) *Diamond Relat. Mater.* **9**, 113–122.
26. Sakaguchi, I., Nishitani-Gamo, M., Loh, K. P., Hishita, S., Haneda, H. & Ando, T. (1998) *Appl. Phys. Lett.* **73**, 2675–2677.
27. Liou, Y., Inspektor, A., Weimer, R., Knight, D. & Messier, R. (1990) *J. Mater. Res.* **5**, 2305–2312.